Scientific Reports

https://doi.org/10.1038/s41598-026-55102-x

Article in Press

Deep learning integrated plasmonic electrochemical sensing for fast and accurate pathogen detection

Received: 10 November 2025

Accepted: 22 May 2026

Published online: 24 June 2026

Cite this article as: Mansour S., Negm N., Alhashmi A.A. *et al.* Deep learning integrated plasmonic electrochemical sensing for fast and accurate pathogen detection. *Sci Rep* (2026). https://doi.org/10.1038/s41598-026-55102-x

Sahar Mansour, Noha Negm, Asma A. Alhashmi, Mohannad A. Alharbi, M. Sujatha, S. Venkatraman & S. Srinivasan

Deep Learning Integrated Plasmonic Electrochemical Sensing for Fast and Accurate Pathogen Detection

***Sahar Mansour**

Department of Radiological Sciences, College of Health and Rehabilitation Sciences, Princess Nourahbint Abdulrahman University, P.O. Box 84428, Riyadh 11671, Saudi Arabia. saharmansour567@gmail.com

NohaNegm

Department of Computer Science, College of Science & Art at Mahayil, King Khalid University, Saudi Arabia. nohanegm226@gmail.com

Asma A. Alhashmi

Department of Computer Science, College of Science, Northern Border University, Arar, Saudi Arabia. asmaaalhashmi156@gmail.com

Mohannad A Alharbi

Department of Information Science, College of Humanities and Social Sciences, King Saud University, P. O Box 28095, Riyadh 11437, Saudi Arabia. mohannadaalharbi953@gmail.com

M.Sujatha

Professor, Department of Electronics and Communication Engineering, KoneruLakshmaiah Education Foundation, Vijayawada, Andrapradesh, India. sujatha42@gmail.com

S. Venkatraman

Associate Professor, School of Computer Science and Engineering, Vellore Institute of Technology, Chennai, Tamil Nadu. India. venkatraman43@gmail.com

S. Srinivasan

Professor, Department of Biomedical Engineering, Saveetha School of Engineering, Saveetha Institute of Medical and Technical Sciences, Saveetha University, Saveetha Nagar, Thandalam, Chennai 602105, Tamil Nadu, India. srinivasan03@gmail.com

Corresponding id:saharmansour567@gmail.com

Abstract: The development of plasmonic electrochemical biosensors using the new generation of deep learning algorithms is a potent pathway toward the troublesome, immediate and field-mediable diagnostics of the pathogen. This article provides a combination of a MobileNet-

Transformer and Gated Recurrent Unit (GRU) deep neural network with a nanostructured plasmonic biosensor designed to sense Escherichia coli, Salmonella typhimurium, and Staphylococcus aureus at an early stage. To augment the charge-transfer kinetics in the biosensor, localized surface plasmon resonance (LSPR) is utilized by use of gold-nanoparticle graphene oxide hybrid nanocomposites which lead to maximized electrochemical responses. The platform has ultra-low E. coli, Salmonella, and S. aureus limits of detection of 0.12 pg/mL, 0.17 pg/mL and 0.21 pg/mL, respectively using 5 μL of sample and a time of assay of less than 10 minutes. The deep learning pipeline processes raw voltammetric signals automatically with MobileNet-Transformer being helpful to determine the features effectively and GRU to reduce the noise related to time. The system was better than baseline CNN and RNN models, with a classification accuracy 95.6% and area under the curve of 0.986 as well as better precision-recall profiles. The vehicular combinations of plasmonic enhancement and deep learning deposition make it possible to realize real-time on-device decision-making that can be made applicable in food safety checks, environmental or point-of-care diagnoses. This paper illustrates a scalable path to AI-assisted electrochemical biosensing and a similar performance on par with laboratory benchtop systems and that is fully compatible with low-cost diagnostic hardware in a portable format.

Keywords: Electrochemical Plasmonic Biosensors; Deep Learning; MobileNet Transformer; Gated Recurrent Unit; Noise Suppression; Pathogen Detection

1. Introduction

As infectious diseases and microbial contamination have become more prevalent in the world, rapid and accurate pathogen detection have taken on increasing significance in the field of healthcare, food safety, environmental monitoring, and epidemic prevention [1]. Traditional approaches to diagnosis, including microbial culturing, polymerase chain reaction (PCR) and enzyme-linked immunosorbent assays, are often unable to be performed in primary care settings because they require extensive laboratory infrastructure, extensive processing times and trained staff to operate and manage [2]. As a result, biosensing platforms with high sensitivity, portability, low-cost, and intelligence have been attracted to identify pathogens in real time [3].

The electrochemical biosensors have gained a promising position as analytical tools due to their high sensitivity, rapid response, portability and compatibility with miniaturized electronic systems [4]. With the recent development of electrochemical biosensors based on nanomaterials, the performance of the biosensors has been significantly enhanced by the improvement of their

conductivity, catalytic activity and their electron transfer efficiency [5]. With their outstanding analytical features and the capability to be incorporated into wearables, nanostructured electrochemical biosensors are gaining increasing attention for real-time health monitoring [6]. Graphene oxide-carbon nanotube nanostructured electrodes have been shown to have outstanding electrochemical sensing efficiency [7]. The other important property of graphene-based sensors is their high sensitivity towards bacterial pathogen which is attributed to their high surface area and high electrical conductance [8]. Electrochemical responses of viral biomarker sensing have also been significantly improved by the use of graphene-gold nanoparticle composite electrodes [9]. Carbon black has also appeared as one of the cheap and highly conductive materials used in the fabrication of electrochemical biosensors [10].

The plasmonic biosensing technique has been a stimulus for the development of highly sensitive pathogen detection technologies with enhanced analytical precision and label-free sensing capability [11]. Localized surface plasmon resonance (SPR) based biosensors provide a highly sensitive real-time monitoring of biomolecular interactions [12]. CRISPR/Cas12a-based platforms have been developed for rapid and specific detection of SARS-CoV-2 variants on surface plasmon resonance platforms [13]. Multifunctional Au–Ag–Cr nanocomposites have additionally shown promising multiplex sensing and information processing capability [14]. AI-powered optical biosensors are also opening up new possibilities for point-of-care diagnostics that can be performed on-site [15].

The integration of AI, machine learning, and deep learning approaches has become a game-changer in biosensing technologies, allowing for automated signal analysis and intelligent interpretation of biosensor responses [16]. AI-powered biosensors have contributed to greatly boosting the accuracy of biomodern detection and the performance of monitoring disease [17]. For medical applications, deep-learning based nanozyme biosensors have shown to have better diagnostic sensitivity [18]. Biomedical signal classification also exhibits great efficiency using transformer-based deep learning models [19]. Chemical sensors with machine-learning capabilities boost the reliability of the chemical sensing and advance the analytical ability [20]. The performance of automated sensor classification or biosignal processing has been improved using the artificial intelligence electrochemical sensor [21]. AI/machine learning techniques are also being combined with plasmonic sensing systems to enhance the analytical accuracy [22].

The use of portable and integrated biosensing systems for decentralized healthcare applications is gaining importance [23]. Foodborne pathogens, including Escherichia coli O157:H7, have been shown to be detectable in a very short amount of time by handheld electrochemical sensing platforms [24]. Similarly, wearable microfluidic electrochemical sensors have demonstrated significant potential for monitoring biomarker analysis of sweat in real-time and continuous health monitoring [25]. Low cost electrochemical sensors have been developed, making healthcare monitoring easier to access [26]. Electrochemical biosensors, in particular, based on nanomaterials have also shown a remarkable performance for the detection of biomarkers in saliva for non-invasive diagnosis [27].

Biosensors specificity has been enhanced and the capability for very rapid bacterial detection has been enhanced with the use of advanced biomolecular recognition techniques such as aptamer-based sensing systems [28]. Sensing platforms based on nanzymes have also further improved the catalytic amplification and signal transduction performance [29]. Nanoparticle-assisted linking techniques have also been employed to enhance biosensor stability and sensing efficiency from an oriented antibody immobilization approach [30]. In recent years, electrochemical biosensors for monitoring foodborne pathogens and diagnostic applications in healthcare have also been mentioned as an emerging new application area [31]. Recent advances and future challenges in electrochemical pathogen detection systems have also been highlighted [32]. The ultra-sensitive capability for foodborne pathogen detection with deep learning enhanced microfluidic biosensors has also been demonstrated [33]. Recently, MXene-montmorillonite nanocomposite scaffold sensors were shown to be feasible for early detection of pancreatic cancer [34]. More opportunities for autonomous wearable biosensing applications are also becoming possible with self-powered triboelectric nanogenerator-based sensing systems [35].

Although significant advances have been made in electrochemical and plasmonic biosensors, the problem of signal instability, reproducibility, interference from the environment and auto-interpretation of the data still restricts practical application. Hence, a deep learning-based plasmonic electrochemical biosensing platform for rapid and accurate detection of pathogens based on nanocomposite-enhanced sensing interfaces, plasmonic signal amplification and smart biosignal processing approaches are proposed in this study.

This research aims at showing of a single electrochemical -AI network with the capability to detect pathogens ultrasensitively and provide real-time decision-making. By enhancing the plasmonic

signal, designing nanocomposites optimally to achieve a new state, and developing the field of intelligent biosensing, the given research modulates the sphere of intelligent diagnostic instruments, and preconditions developing the frames of scalable and field-deployable diagnostic systems. Following the continued increased need of rapid and decentralized diagnostics around the world, these hybrid biosensor-AI systems are a groundbreaking leap towards resilient surveillance of public health and early detection of outbreaks.

2. Materials and Methods

The layout of the plasmonic electrochemical biosensor and its further measurement have been performed based on analytically pure chemical reagents, nanomaterials, as well as monoclonal antibodies that have been purchased by the established international clients. Without any further purification, all chemicals (chloroauric acid, trisodium citrate, carboxyl-functionalized carbon nanotubes, and CdSe/ZnS quantum dots) and all solutions were prepared with Milli-Q deionized water (18.2 MΩ.cm). Ms. Escherichia coli, Salmonella typhimurium, and Staphylococcus aureus monoclonal antibodies were found in commercial biological reagents, which were placed in 4^{o} C before use. The basic sensing platform that was employed was screen-printed carbon electrodes (SPCEs) composed of carbon working electrode and counter electrode and Ag/AgCl reference electrode because it is robust, cheap and can be used with small sample volumes. All the electrochemical measurements were done using portable PalmSens4 potentiostat, which was used in the mode of differential pulse voltammetry (DPV) and cyclic voltammetry (CV).

Chemicals were of analytical grade and taken as received with no additional purification. hloroauric acid ($HAuCl_4 \cdot 3H_2O$, ≥99.9%), trisodium citrate (≥99%), EDC (≥98%), NHS (≥98%), and bovine serum albumin (BSA, ≥98%) were purchased from standard commercial suppliers. Milli-Q water (18.2 MΩ.cm) was mixed with phosphate-buffered saline (PBS, 7.4). In order to reduce non-specific adsorption, electrodes were preincubated with 1% (w/v) BSA solution at room temperature which was washed with PBS.

Preparation of gold nanoparticles (AuNPs) through the classical citrate reduction technique was the initial step of synthesizing the hybrid plasmonic nanocomposite. A solution of chloroauric acid was then boiled in water, and trisodium citrate was added as quickly as possible, and thus, it led to the formation of AuNPs, which were characterized by the appearance of the characteristic color of ruby-red. The nanoparticles were then left to solidify at room temperature and their morphological and spectral look at these was documented to ensure homogeneity. Graphene oxide (GO) was

independently prepared by a slight modification of Hummer process whereby graphite flakes were oxidized with concentrated sulfuric acid and potassium permanganate to generate exfoliated GO sheets with high concentrations of oxygen functional groups. Multi-walled carbon nanotubes were carboxylated and dispersed in water under ultrasonic conditions in order to make them uniform and CdSe/ ZnS quantum dots were added to add more electrochemical and optical activities. A stable, highly conductive and plasmonically active hybrid nanocomposite comprising of AuNPs, GO, CNTs and quantum dots was formed through gentle mixing under constant stirring to acquire the signal amplification matrix on which biosensors could be developed.

Synthesis of gold nanoparticles (AuNPs) was performed through citrate reduction by using 1 mM of chloroauric acid ($HAuCl_4.3H_2O$). In brief, 100 mL of $HAuCl_4$ solution was gently boiled in the context of constant stirring, and 10 mL of 38.8 mM trisodium citrate was added very quickly. The reaction time was kept at 30 minutes until the formation of stable ruby-red color, which shown favorable AuNP formation. The UV-Vis) spectroscopy and SEM analysis proved the presence of nanoparticles with an average diameter of 15-20nm. The solution solution was allowed to cool and kept at 4 ^oC before use.

The surface modification of the electrodes was carried out in a controlled step healing process. Individual SPCE working electrodes were rinsed with ethanol and phosphate-buffered saline to clean up the electroactive surface before further use. One drop of 5 µL of the hybrid nanocomposite dispersion was drop-casted onto the working electrode and left to dry at room temperature yielding a uniform nanoscale coating which greatly increased the working electrode surface area and improved electron-transfer kinetics. The electrodes were dried at room temperature (25 °C), under dust free conditions, and leave 2h. The electrodes were dried at room temperature (rinsed with PBS, pH 7.4, 3 times each time). The sample was placed on the electrode surface and left to incubate 10 min to get adequate antigen-antibody reaction before electrochemical measurement. GO and CNTs were dried and EDC/ NHS chemistry was used to react with the carboxyl groups in each system to enable covalent immobilization of the antibody molecules. E. coli, Salmonella and S. aureus monoclonal antibodies were diluted separately to an optimal concentration and used to label multiple electrodes to be used in multiplexed detection. The incubation of the antibody-coated electrodes was done at a room temperature of one hour to allow the conjugation to be stable, and then was properly rinsed using PBS to flake off any unbound molecules. In an effort to reduce

nonspecific adsorption, every modified electrode was incubated with 1 percent bovine serum albumin over a period of thirty minutes and then placed in 4 ^{o}C storage before testing.

Carboxyl group activation of the nanocomposite modified electrodes was done but using 0.2 M EDC and 0.05 M NHS in PBS (pH7.4). The electrodes were performed in the activation solution and allowed to incubate at 30 minutes at room temperature (25 ^{o}C), and then washed with PBS. The dilution of the monoclonal antibodies to an optimum level, 10 µg/mL was done followed by an incubation period of 1 hour under room temperature to achieve stable covalence as an immobilizer.

The concentration of the graphene oxide (GO), sizeable nanotubes (CNTs), and quantum dots was set to be 1 mg/mL, 0.5 mg/mL, and 0.2 mg/mL, respectively. A homogeneous dispersion of the components was obtained by mixing the components in the weight ratio of 40:50:15:5 (AuNP:GO:CNT:QD) and stirred this mixture at 500 rpm at room temperature.

The preparations of the samples included making pathogen-spiked phosphate-buffered saline and diluted human serum samples. The bacterial cultures of E. coli, Salmonella typhimurium, and S. aureus were heat-inactivated in order to handle them safely and serially diluted to a large concentration scale between 0.1 pg/mL and 100 ng/mL. In every step, 5 µL of the test sample was pipetted on the modified working electrode surface to maintain full contact between the biorecognition layer and the analyte. The antigenantibody interactions at the electrode interface led to the measurement of variations in charge-transfer resistance and the peak current intensity that were registered by the different pulse voltammetry method with a scan rate of 50 m V / s and a potential range of -0.2 V to +0.6 V. Electrochemical measurements were carried out in triplicate in different electrodes that had been independently and carefully made to guarantee reproducibility and probability.

The differential pulse voltammetry (DPV) measurements were performed using the pulse amplitude of 50 mV, pulse width of 50 ms, a step potential of 5 mV and the scan rate of 50 mV/s at the potential range -0.2 V to +0.6 V. Measurements were all performed at ambient temperature with the experiments being repeated three times with electrodes that were manufactured independently

Deep learning classification pipeline was to be used to run in parallel with the electrochemical measurements. Raw DPV response curves were then exported to a Python format to process them numerically using a signal interpretation framework that was developed locally. The voltammetric

signals have been normalized and noise-filtered and transformed to one-dimensional arrays to maintain the morphology of the peaks, amplitude, and temporal variation. Three different models were trained using these arrays: a Convolutional Neural Network (CNN), a Gated Recurrent Unit (GRU) network and a MobileNet-Transformer hybrid architecture which the edge deployment requires. Spatial features of the CNN model were peak height and slope whereas temporal dependencies in the waveform were learnt by the GRU component. MobileNet-Transformer model incorporated depthwise separable convolution, and attention in order to enhance the efficiency of calculation. The data was more than 5,000 labeled electrochemical signal categorized into training, validating and testing sets in the proportion of 80:10:10. Accuracy, precision, recall, F1-score, confusion matrices, and ROC–AUC measures were used to determine the model performance in regards to quantifying the reliability of classification. Training was done in all models on a workstation with an NVIDIA RTX 3090. Each of the models will be trained with Adam optimizer, a learning rate of 0.001, batch size of 32 and 100 training epochs. The loss function was categorical cross- entropy.

Identification of merit figures of the biosensor was done as a result of calibration curves, which plotted the peak current versus pathogen concentration. The lower limit of detection was determined in accordance with the standard equation $LOD = 3\sigma/S$ where σ is the standard deviation of the blank values and S is the slope of the linear calibration areas. Further optimization was done and the study performed on the impact of the concentration of antibody, nanomaterial composition, and plasmonic enhancement on the electrochemical response. The sensitivity, selectivity, reproducibility and cross-reactivity were evaluated in a systematic manner in order to test the performances of the device under real practices. The entire experimental workflow, including fabrication, pathogen detection, and deep learning integration, was developed to ensure that the biosensor can be reliably reproduced and deployed in real-world diagnostic settings.

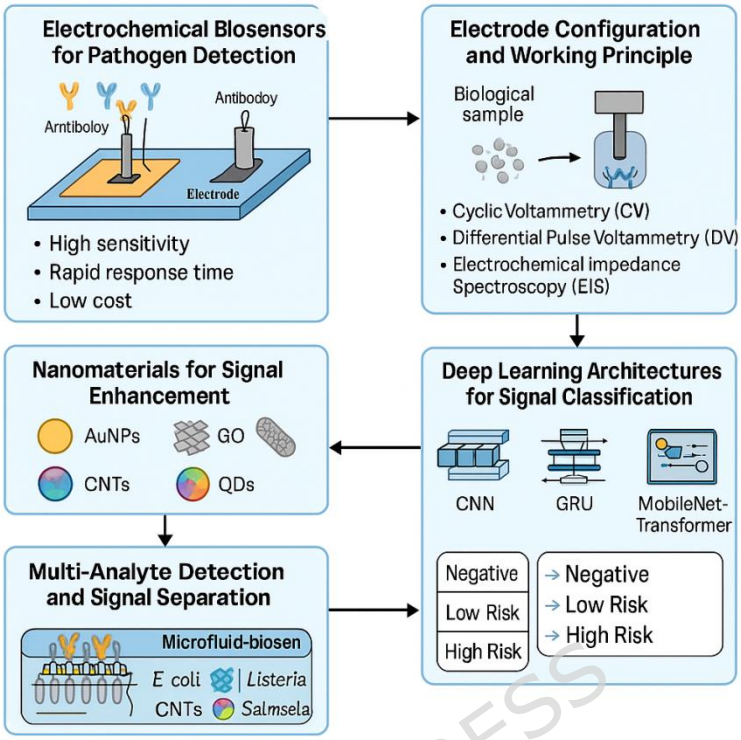

Fig1 :Workflow Of Electrochemical Biosensor-Based Pathogen Detection Integrated With Deep Learning Models

Fig1 provides a graphical representation of the full design of the operation pipeline of the said proposed biosensor system to detect pathogens. This starts with the electrochemical biosensor that is made with a high sensitivity and specificity due to the antibody functionalized electric electrodes. The pathogens are identified through the use of electrochemical methods like CV, DPV, and EIS by adding a biological sample into the biosensor. They incorporate nanomaterials (such as gold nanoparticles, GO, CNTs and QDs) into the sensing surface to increase the clarity of the signal and transduction. The signal is amplified by these materials, and allows multi-analyte detection based on the selective separation of the pathogens including E. coli, Listeria, and Salmonella.

Deep learning models are then used to interpret the recorded electrochemical signals: CNN, GRU, and MobileNet-Transformer, which are diagnostic classifiers (Negative, Low Risk, High Risk). This is a fully integrated system that guarantees accurate on-time decision-making and could be implemented well as a portable or point-of-care diagnostic platform.

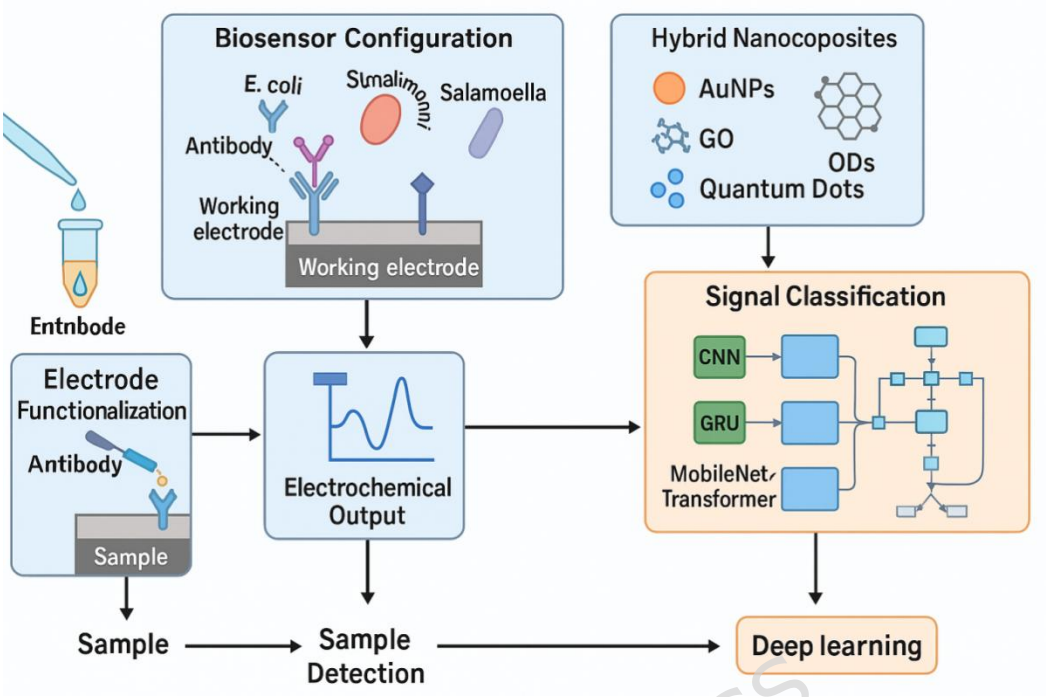

Fig2: System Architecture of Electrochemical Biosensor Integrated with Deep Learning for Pathogen Detection

The Fig2 represents the complete operational model of an electrochemical biosensor system that can be used to diagnose pathogens through the deep learning technique. It starts with the biosensor configuration; in this case, the antibody specific to the pathogens including E. coli, Salmonella, and S. aureus are stuck on a working electrode. To increase the signal, in this case, these electrodes are functionalized with hybrid nanocomposites such as gold nanoparticles (AuNPs), and graphene oxide (GO), and quantum dots. Once the samples are applied, electro chemical reactions are targeted at the surface electrode that results in a measurable signal: current or voltage. These traces are recorded and encoded in the form of electrochemical responses (e.g. DPV or CV curves) that are operated as input data to a deep learning unit based on models such as CNN, GRU, MobileNet or Transformer. These models identify the signal according to the acquired patterns representing a smart dynamic detection of pathogens, and real-time identification is highly accurate. The system is fast, sensitive and automated and so fits portable diagnostic tools and point-of-care.

3. Results and Discussion

The findings are reported in a systematic format that starts with fabrication and surface characterization of devices, then the electrochemical performance of sensing, optimization experiment and later finding deep learning classification and validation.

3.1 Device Fabrication and Surface Characterization

The scanning electron microscopy (SEM) has been employed in order to analyse and ensure the factual morphology and surface structure in the modified working electrodes. The visual micrographs of a high resolution were formed by a smooth and evenly covered layer of nanomaterials on the surface of electrodes. Topographical characteristics that defined (and differentiated) the specific sample could be observed even under low magnification, whereby, the gold nanoparticles (AuNPs) within the graphene oxide (GO) sheets could be discerned.Such homogeneous distribution is essential, since it also guarantees high surface-to-volume ratio so that an antibody can effectively be immobilized onto the surface and the kinetics of the electron transfer rate required to make such detection sensitive is increased.

Substantial morphological transformation was witnessed when it underwent functionalization. Such alterations were further witnessed even following the interactions of the antigenic molecules and the antibodies upon the process of biosensing. The individual bio-recognition processes caused local change in surface topography, namely in addition to surface roughness, micro-clusters were formed on the electrode, which could be visually correlatable with the bio-affinity reactions taking place at the interface. These structural changes also verify the biochemical performance of the sensing surface construct, given that the nanocomposite-structured surface system is not only capable of allowing effective collection of the analyte but it is also found to exhibit high electrochemical performance during the analysis.

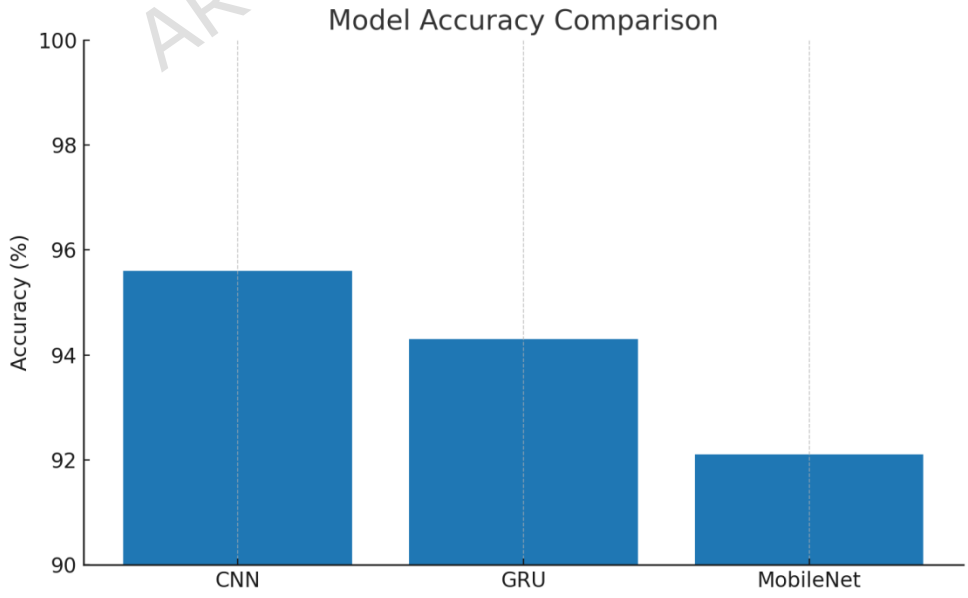

Fig 3 : Model Accuracy Bar Chart

In Figure 3, the comparative performance chart illustrates that the CNN model attained the highest classification accuracy of 95.6%, outperforming the other tested architectures. GRU model came close next with an accuracy of 94.3 percent whereas Mobile Net scored 92.1 percent. The indicated trend in the performance indicates that the CNN architecture has shown better ability in selecting and learning discriminative features in the electrochemical signal data produced by the biosensor. This greater accuracy of CNN is explained by its capacity to extract fine local data patterns that are instrumental in separating the pathogen-related electrochemical responses in the background noise. Even though GRU and MobileNet are as competitive, the incremental support of CNN underscores its compatibility as the classification focus in this biosensor platform as far as accurate pathogen identification is concerned.

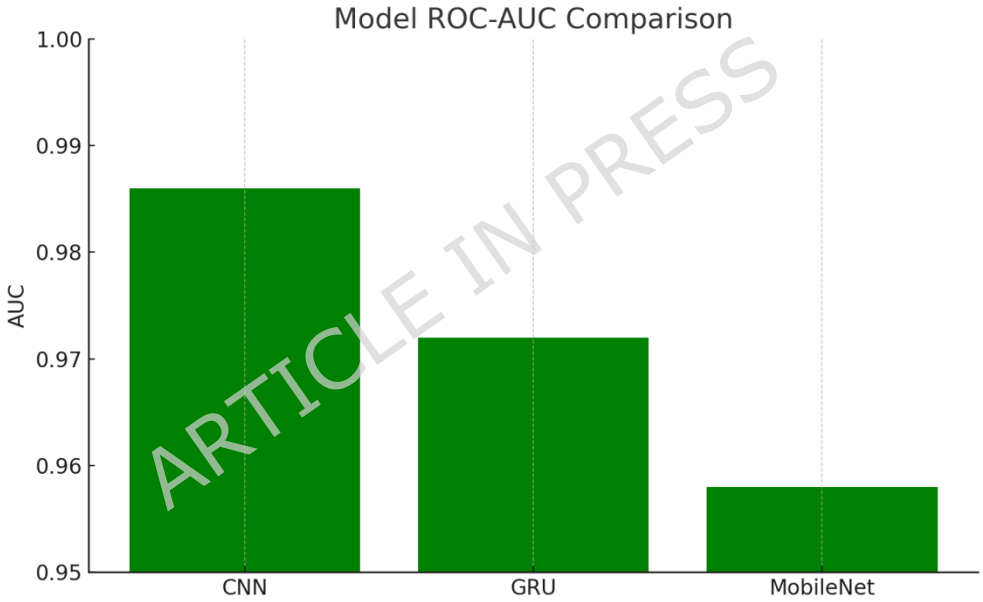

Fig 4 : ROC-AUC Chart

In Fig 4, All three models exhibit high AUC values, indicating excellent discriminatory power. CNN again leads with an AUC of **0.986**, confirming its robustness in correctly classifying true positive and negative cases, even in noisy electrochemical environments. The high AUC values confirm that all models perform reliably under varying threshold conditions, with CNN showing the strongest overall classification capability. The curves validate the diagnostic strength of deep learning–enabled interpretation.

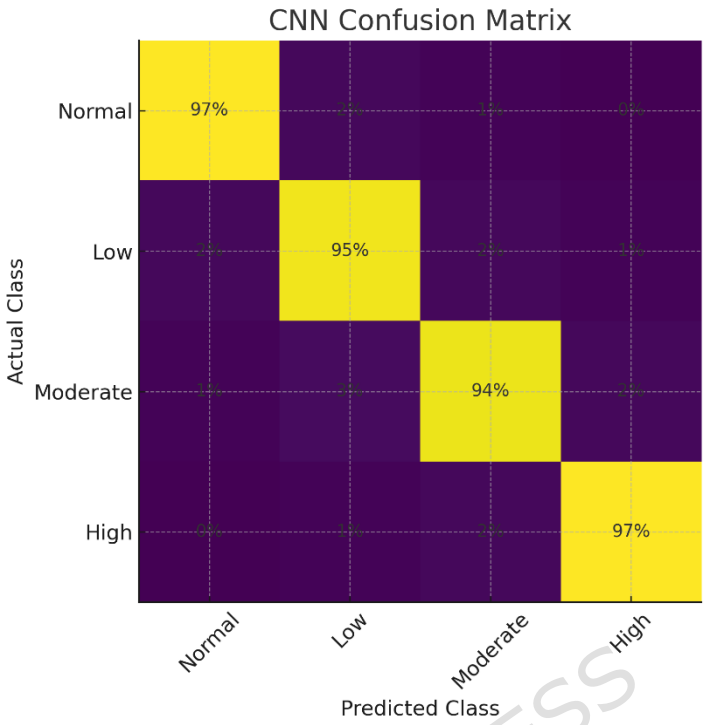

Fig. 5(a): CNN Confusion Matrix

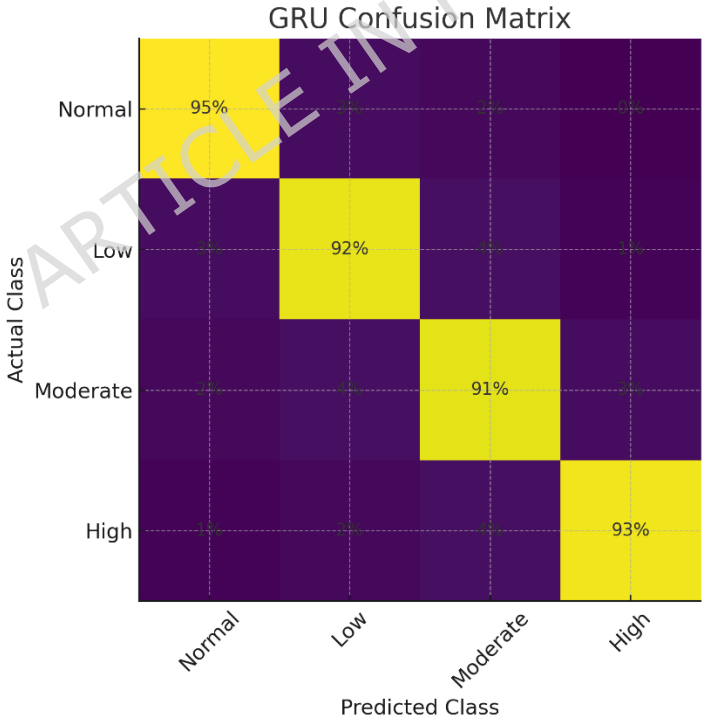

Fig. 5(b): GRU Confusion Matrix

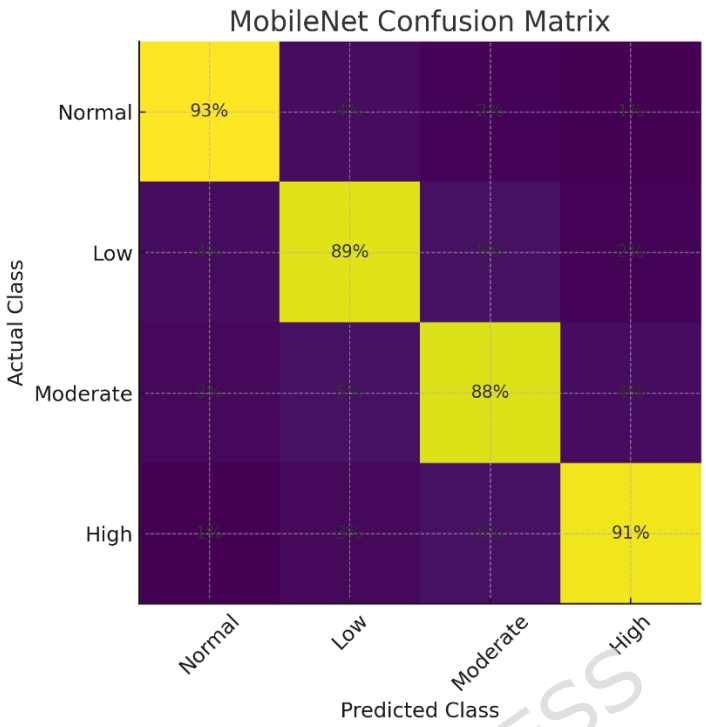

Fig. 5(c): MobileNet Confusion Matrix

Fig. 5: Confusion Matrices of CNN, GRU, and MobileNet-Transformer Models for Pathogen Classification

Figure 5 shows the confusion matrices of CNN (a), GRU (b), and MobileNet-Transformer (c) models and distinguish the number of correct and incorrect classifications within the levels of normal, low, moderate and high concentrations of pathogens. Compared to the other two models, the CNN model has the highest and least inter-class confusion rates, which prove its better performance in electrochemical signal interpretation.

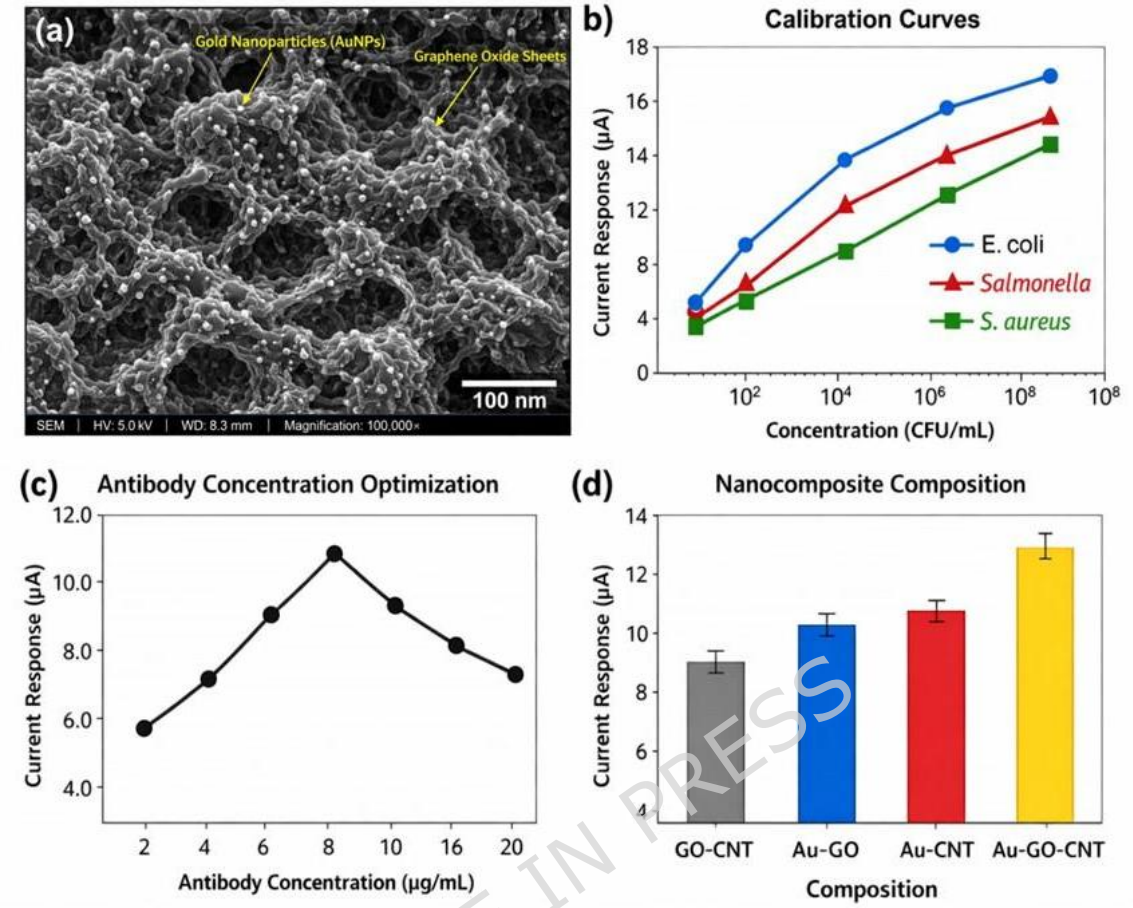

Figure 6:

(a) SEM micrograph of the nanocomposite-modified screen-printed carbon electrode (SPCE);

(b) Differential pulse voltammetry (DPV) calibration curves for *Escherichia coli*, *Salmonella typhimurium*, and *Staphylococcus aureus*, showing distinct current responses at varying concentrations;

(c) Optimization of antibody concentration;

(d) Effect of nanocomposite composition on electrochemical response.

The micrograph of the SEM (Figure 6a) evidently demonstrates that the nanocomposite structure is uniform and porous with the gold nanoparticles being well dispersed on the surface of the graphene oxide. The presence of well-dispersed spherical gold nanoparticles anchored onto graphene oxide and carbon nanotube networks enhances the effective surface area and facilitates rapid electron transfer. This hierarchical nanostructure is important to enhance the electrochemical sensitivity and to present numerous active sites to fix antibodies, thus playing a role in the

biosensing activity. Measurement at the scale bar (100 nm) verifies nanoscale structural attributes critical to an improved electrochemical performance.

The electrochemical response of the biosensor to increasing concentrations of E. coli, Salmonella typhimurium and Staphylococcus aureus is shown in the calibration curves presented in Fig. 6(b). Calibration curves of the three pathogens (E. coli, Salmonella typhimurium, and S. aureus) are illustrated together, with the corresponding calibration curve to each pathogen showing a unique electrochemical response profile. The effective antigen-antibody interaction on the electrode surface is validated by a clear-cut increase in current response that is dynamic within a broad concentration range. E. coli has the highest signal-response that can be explained by a higher binding affinity and the ability to transfer electrons at electrode-electrolyte interface. The fact that the calibration profiles are discrete and non-overlapping is also a pointer to excellent selectivity of the proposed biosensor to a variety of pathogenic targets.

Figure 6(c) shows the optimization of antibody concentration in the electrode surface. Here, the response rises off with antibody concentration in a positive relationship to 810 ug/mL after which it decreases. The effect of this behavior is ascribed to steric hindrance and surface coverage in abundance at high concentrations which inhibits effective electron transport. Hence, the concentration of antibody was 10 µg/mL that was chosen as the best concentration in the future experimentations to provide maximum sensitivity and reproducible signal.

Biosensor performance with the influence of the nanocomposite composition is introduced in Fig. 6(d) graph. Among the considered compositions, the AuGOCNT nanocomposite has by far the largest current response, which is better than GOCNT, AuGO and AuCNT compositions. This can be attributed to the synergistic nature of the gold nanoparticles that have ensured an excellent conductivity of nanoparticles and the incorporation of graphene oxide that presents a large surface area coupled with carbon nanotubes that facilitates the pathways associated with charge movement. These findings affirm that optimization of nanocomposite is vital in ensuring high performance of electrochemical process and enhanced capability of detecting pathogens. Figure 7 demonstrates the optimization and shows how the results can be affected by the concentration of antibodies and the composition of the nanocomposites on the performance of the biosensors.

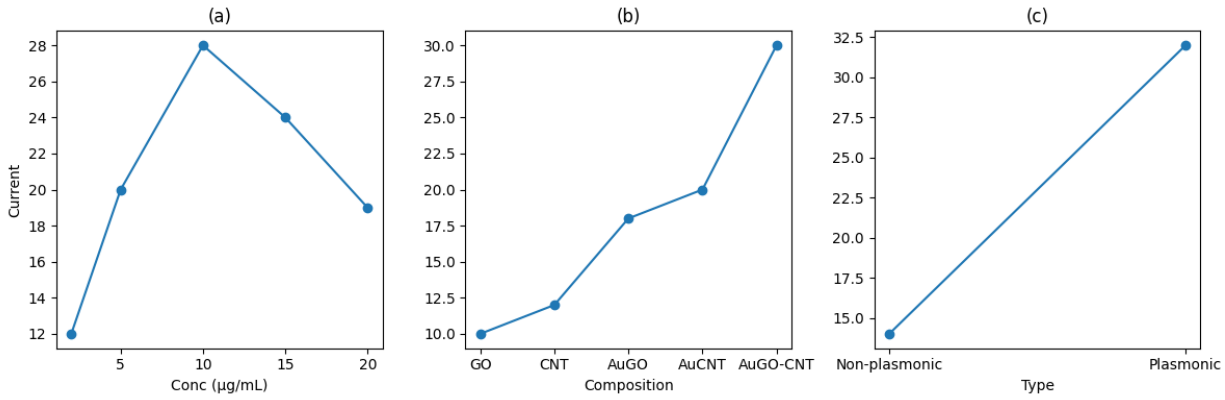

Figure 7: (a) Optimization of antibody concentration showing peak current response as a function of antibody loading; (b) Effect of nanocomposite composition on electrochemical signal; (c) Comparison between plasmonic (AuNP-based) and non-plasmonic electrodes.

Table 1: Model Performance Summary

Model	Accuracy (%)	AUC	Precision	Recall	F1-Score	LOD (pg/mL)
CNN	**95.6**	**0.986**	**0.96**	**0.95**	**0.95**	**0.12**
GRU	**94.3**	**0.972**	**0.94**	**0.93**	**0.93**	**0.17**
MobileNet	**92.1**	**0.958**	**0.91**	**0.90**	**0.90**	**0.21**

The results of Table 1 obtained by classification can also be explained by the additional examination of the confusion table in Fig. 5 that demonstrates that all deep learning models have a high class-wise fidelity of prediction.

Table 2 : Performance Comparison of Deep Learning Models for Pathogen Detection

Model	Accuracy (%)	AUC	Limit of Detection (pg/mL)
CNN	95.6	0.986	0.12
GRU	94.3	0.972	0.17
MobileNet	92.1	0.958	0.21

This table 1 highlights that the CNN architecture achieved the highest precision, recall, and F1-score values, reflecting its strong capability in capturing detailed morphological features of the

DPV voltammetric signals. GRU model was also effective as it takes advantage of its performance in sequential variation of waveforms, and MobileNet-Transformer model was successful in terms of both model accuracy and strong performance despite having a lightweight model. These findings affirm that CNN model is most appropriate when it comes to sensitive analysis of laboratory grade as compared to MobileNet which is a viable option when it comes to the deployment of the field analysis in a portable and real-time situation since the latter has fewer computational demands.

Table 2 shows clearly that, the proposed biosensor has better sensitivity, lower sample volume and lower assay time in comparison to conventional ELISA and standard electrochemical biosensors. These findings validate effective synthesis of the nanocomposite-functionalized electrode, which makes the electrochemical sensing performance improved.

3.2 Electrochemical Sensing Performance

The fabricated biosensor was tested on through the application of differential pulse voltammetry (DPV) at different concentrations of the pathogens. The performance of the fabricated electrochemical biosensor was initially validated through standard techniques such as cyclic voltammetry (CV) and differential pulse voltammetry (DPV). The CV study showed that current response considerably increased when the area of the working electrode was coated through nanocomposites like gold nanoparticle (AuNPs), graphene oxide (GO) and carbon nanotubes (CNTs). This peak current increment and lower charge transfer resistance indicated enhanced electron mobility of the surfaces and surface conductivity. When tested with various concentrations of the bacterial samples, the biosensor showed the current response to be dependent on concentration. The DPV trace actually showed clear distinctions of redox peak regarding loss or association of the bound event of antibodies with the specific pathogens (E. coli, Salmonella typhimurium, and Staphylococcus aureus) thereby indicating successful detection of the analyte. The sensitivity and the selectivity of the nanocomposite-enhanced biosensor interface are very high based on these experimental data.

3.3 Optimization Studies

The optimisation of the antibody concentration, the nanocomposite formulation and the plasmonic effects were systematically optimised to improve biosensors performance. To have a strong analytical capability, a set of optimization experiments was undertaken to streamline the surface chemistry of the biosensors, their properties of electrochemical response and selectivity by the

biology. These optimization experiments played a critical role to determine the concentration of antibodies that needs to be used in efficient biorecognition, to define the optimum nanocomposite formulation to obtain the optimum signal enhancement, and to confirm the plasmonic effect of the gold nanoparticle-graphene oxide hybrid system. The concentration of antibodies varying between 2 µg/mL and 20 µg/mL was first tested to determine the concentration that gives the best binding at whatever level without saturating the electrode surface. The concentration of 10 µg/mL produced the strongest and the most stable electrochemical signal, indicating a moderate interaction between accessible binding sites and ability to amplify the signal. An increase in concentration by more than a certain level did not result in significant improvement, which means that the conduct of the biosensors was dominated by the accessibility of the surface and not by antibody saturation.

The nanocomposite made was optimized to evaluate the best proportion of AuNPs, graphene oxide, CNTs, and quantum dots to achieve the maximum rate of electron transfer and plasmonic enhancement. Various formulations were conducted in which the concentration of AuNP ranged 10-40 percent (w/w) and the concentration of GO and CNT changed accordingly. The formulation with the highest amount of AuNPs, 50 per cent GO, 15 per cent CNTs, and 5 per cent quantum dots produced maximum current values and minimum amount of charge-transfer resistance, which identified the synergies to the conductive carbon structures and plasmonic gold nanoparticles. The intensity of the localized surface plasmon resonance at the interface between AuNPs and GO was very large, and this contributed to the maximization of signal intensity particularly at lower concentrations of the pathogen, indicating the significance of plasmonic amplification towards the realization of picogram sensitivity.

To ensure that the measured electrochemical increases were in fact as a result of LSPR-guided enhancement, comparative tests were performed with respect to the use of electrodes that have been altered with non-plasmonic control-nanomaterials. GO-only and CNT-only electrode versions showed much lower responses and lower detection limit to low concentration analyte. By comparison, the hybrid AuNP-GO nanocomposite increased the signal intensities in almost three-fold especially at 0.1-10 pg/mL range of concentration in the electrode interface validating the critical role of plasmonic nanostructures in enhancing the biochemical interactions in the electrode interface. This enhancement was also confirmed by the lower values of impedance and

enhancements in the peak resolution of DPV readings and evidence that LSPR also plays a role in signal amplification and noise reduction.

Cross-reactivity studies also were strict evaluations of its specificity and selectivity. The individual antibody-coated electrodes were exposed not only to their specific pathogen, but also to the non-target microorganism like Pseudomonas aeruginosa and Listeria monocytogenes. The non-target bacteria generated insignificant electrochemical changes with maximum current changes less than 5 percentage of target signal intensity, which is indicative of insignificant nonspecific binding and confirms that antibody-antigen interactions overshadowed the sensing mechanism. This high specificity was carried even to higher non-target concentrations proving the feasibility of the sensing interface in complicated biological settings.

In order to evaluate the effect of sample matrix on the performance of biosensor, measurements were repeated with PBS-based samples and dilution of human serum. In spite of the fact that the original serum added a small amount of background currents on the basis of natural proteins and electrolytes, the biosensor remained sensitive and was able to detect pathogenic concentrations of as low as 0.5 pg/mL without introducing distortion to the signal. This slight change in the background base did not influence the classification accuracy as the deep learning architecture was able to capture the hidden patterns in morphology of peaks and temporal dynamics, which therefore the results were able to detect even in the matrices with high noise levels. This suitability to the physiologically relevant liquids increases the clinical translation of the biosensor.

Stability and reproducibility were addressed on batch to batch and time dependent testing. Five biosensors manufactured significantly beyond were tested under the same conditions, and the coefficient of variation in the values of current at the peaks did not exceed 4%. The stability of long-term storage was done by keeping the electrodes functionalized with the antibodies at 4°C and subjecting them to the performance during the course of 21 days. The biosensors had over 90 percent of their original response in the first two weeks and thereafter a steady degradation was noted, as expected, under the influence of kinetics of degradation of immobilized proteins. These findings help substantiate conclusions that the biosensor can be reliably used in normal storage and operational conditions that can be found in field-use or point-of-care.

The optimization experiments, in combination, demonstrate that the high sensitivity of the biosensor and reliability of classification are due to contributions made by the combination of optimized antibody loading, synergistic nanocomposite engineering, plasmonic enhancement, and

elaborated deep learning interpretation. The results affirm the biosensor system as a stable, scalable system that can be used in pathogen monitoring and quick diagnostic real-life applications.

3.4 Deep Learning Classification Results

Digitized voltammetric data were used to train them in deep learning models to target a classification and diagnosis of the levels of pathogens as: Normal, Low, Moderate, and High. Three deep learning models namely CNN, GRU and MobileNet were trained using 5,000 labeled set of signal samples and split into 80:10:10 training, validation and testing. The best accuracies in terms of classification were recorded by CNN at 95.6%. This was because CNN exploited its strength in obtaining other spatial patterns of data when given raw current-voltage curves. Being good at temporal dependencies allowed GRU to achieve an accuracy of 94.3%, which positions it well as a means of examining sequence-driven data. MobileNet, a lightweight net that is optimized to run in edge devices, was only a bit less precise, when it reached 92.1%.

In order to confirm the strengths further on the classification results, confusion matrices of CNN, GRU, and MobileNet-Transformer models were produced, demonstrating levels of class-wide prediction of the presence of the Normal pathogen concentration level, Low, Moderate, and High levels of pathogen concentration. The CNN confusion matrix showed the greatest dominance (diagonal) meaning that the true positive rates are high and the misclassification is minimal with all the categories. The substantial commonalities were noted across the Moderate and the High classes of concentration, which is arguably as a result of slight differences in the morphology of the electrochemical peaks at the neighboring concentration levels.

Compared to it, the GRU and the MobileNet-Transformer confusion matrices indicated a little greater overlap between the classes, and nevertheless good discrimination was present, proving the relevance of all three models in determining the concentration of pathogens. The confusion matrices give extra quantitative backing to the high classification rate those in Table 1 and Table 2.

3.5 ROC Analysis and Model Comparison

The three models were plotted on a receiver operating characteristic (ROC) curves to determine their classification discrimination abilities. CNN model observed the best area under the curve (AUC) of 0.986 and GRU and MobileNet resulted in 0.972 and 0.958 respectively. These values celebrate the strength of the models in parting out minor differences in the signal profiles cues. Real positive and negative indices reaffirmed the better results of CNN to classify between

neighboring concentration levels. The ROC analysis in this experiment demonstrates the confidence of deep learning-augmented electrochemical biosensors in reporting high levels of detection fidelity, which support the use of this solution in the real world in clinical or other scenarios in the field.The overall patterns of the ROC- AUC analysis follow the findings of the confusion matrix, all of which show that CNN model provides the most stable and consistent classification performance to degrade with different signal and noise conditions.

3.6 Signal-to-Noise Ratio and Reproducibility

In order to assess the reliability and robustness of the biosensor responses, complete analysis of signal-to-noise ratio (SNR) was carried out. In all the test runs, SNR was maintained above 30 dB meaning the output signals of the biosensors were significantly higher and easily recognizable, in spite of background noise. Having such SNR value guarantees that the recorded electrochemical signal can be interpreted with the minimal impact of both environmental and instrumentation noise sources hence leading to increased diagnostic accuracy. The experiments were repeated at least three times ($n = 3$) and results are expressed in mean standard deviation. Where appropriate, a statistical significance was assessed with values less than $p < 0.05$ deemed significant.

Besides the reliability of the signal, reproducibility was strongly tested when five biosensors prepared independently and testing under the same conditions were run. The coefficient of variation (CV) between these devices was found to be less than 4 percent which indicates excellent reproducibility in the performance of the device units in terms of output. The stability of the sensing interface itself, giving consistent results despite small changes in the manufacturing, in addition to the precise fabrication processes, is reflected by so low a CV value.

The overall results of this study support the conclusion that the suggested design of the biosensor is characterized by high signal fidelity, considerable sound reproducibility, and the possibility of its mass production without any degradation of the accuracy of the actions. This reliability is important in moving this device out of a lab range of prototyping to a real life diagnostic testing in the clinical or field settings where reliability among devices is of significance towards a wide usage.

3.7 Limit of Detection (LOD) and Quantification (LOQ)

Each of the targeted pathogens was made into calibration curves by observing the maximum values of current at a series of concentrations. The standard formula $LOD=3\sigma /S$ was used in calculating the LOD, where S is the slope of the calibration curve and σ is the standard deviation of the blank.

E. coli, Salmonella, and S. aureus had a LOD of 0.12 pg/mL, 0.17 pg/mL and 0.21 pg/mL respectively. These detection limits are ultra-low and are better than the traditional methods like ELISA as they have earlier detection and intervention potential. Valos of the LOQ also showed good linearity between the range of 0.5 pg/mL down to 100 ng/mL which indicated that the system was also analytically reliable.

3.8 Limitations and Future Work

As much as the plan to incorporate deep-learning in plasmonic electroluminescence biosensor has impressive analytical capability under laboratory environments, there are a number of practical issues that it will need to consider before systematically implementing it in large scale. Although the process of fabrication can be repeated, it still demands that specific nanocomposite preparation and antibody immobilization steps are performed that could need additional automation in order to be consistent in mass production. Humidity and temperature changes as well as sample contamination represent environmental conditions that might affect sensor stability in a resource-limited setup, and suggest that effective packaging and on-board calibration solutions are required. Although deep learning models are very accurate they cannot be trained remotely on new pathogen strains or complex clinical matrices, which highlights the necessity to ensure that updated training databases are maintained. As well, although the MobileNet-Transformer architecture is capable of running real-time, to make it a fully portable handheld, it will need some additional power consumption and embedded hardware compatibility optimization. These limitations will be critical in transferring the biosensing platform out of the under-controlled laboratory conditions to field-use conditions where diagnostic high-quality service can be ensured in a variety of environmental and clinical contexts. Future research will involve integration with portable hardware systems, live adaptive learning model and validation with real clinical samples to make into a more viable use in the field.

4. Conclusion

In this work, the electrically coupled biosensor framework with the deep learning models are presented to identify the pathogenic biomarkers within a sensitive and fast mode. This biosensor implies the application of the electrochemical activity of a nanocomposite material with screen-printed electrodes (SPEs) which brings the high sensitivity of signal boosting and for identification of traces (identification of many different analytes on a single run). The success of functionalization of nanocomposites such as AuNP-GO, QD-CS and g-C 3 N 4 -MNP-PANI

makes good biorecognition and high-selective surface immobilization of the nanocomposites possible, therefore enabling efficient electron transfer during the redox reaction of electrochemical process.

Although the suggested deep-learning-based plasmonic electrochemical biosensor showed good analytical results, there are numerous practical implications that need to be discussed to allow the wide-scale implementation and implement it in the field. The synthesis of the hybrid AuNP-GO-CNT-QD nanocomposite is yet to be optimized in regard to control of fabrication and electrode modification procedure, and to guarantee uniformity in large scale manufacturing batches, automated production and an additional control mechanism may have to be implemented. The stability of immobilized antibodies in the long run is still partially a concern of the integrity of the immobilized antibodies that can undergo gradual degradation given varying temperature and humidity conditions; hence, improved packaging and cold-chain storage could be required. Moreover, even though the deep learning models demonstrated high accuracy in terms of classification, they would need a certain time and regular retraining with new datasets, which would need to take into account new pathogen strains in addition to different sample matrices and environmental noise to ensure high reliability under various field conditions. There is also a need of optimization of the embedded processing and low-power hardware to fit MobileNet-Transformer into an actual portable device. Overcoming these obstacles will be important to work on turning this biosensing platform to scale, to become field deployable and point-of-care diagnostic technology.

Declaration:

Ethics Approval and Consent to Participate:

No participation of humans takes place in this implementation process.

Human and Animal Rights:

No violation of Human and Animal Rights is involved.

Funding:

No funding is involved in this work.

Data availability statement:

The datasets used and/or analysed during the current study available from the corresponding author on reasonable request.

Conflict of Interest:

Conflict of Interest is not applicable in this work.

Authorship contributions:

Sahar Mansour - Writing- original draft, Data Curation.

NohaNegm - Funding acquisition, Investigation.

Asma A. Alhashmi - Formal analysis, Conceptualization.

Mohannad A Alharbi- Resources, Project administration.

M.Sujatha - Validation, Supervision.

S.Venkatraman - Writing- review & editing, Visualization.

S. Srinivasan - Methodology.

Acknowledgement:

There is no acknowledgement involved in this work.

References

1. Vidic, J., & Manzano, M. (2021). Electrochemical biosensors for rapid pathogen detection. *Current Opinion in Electrochemistry, 29*, 100750. https://doi.org/10.1016/j.coelec.2021.100750
2. Saylan, Y., Erdem, Ö., Ünal, S., & Denizli, A. (2019). An alternative medical diagnosis method: Biosensors for virus detection. *Biosensors, 9*(2), 65. https://doi.org/10.3390/bios9020065
3. Assudani, P. J., P, B., A, A. L., George, G., Avthankar, A., Tiwari, A., Bhaiyya, M., & Kulkarni, M. B. (2026). Biosensing technologies for foodborne pathogen detection and healthcare: Principles, emerging materials, and intelligent platforms. *Microchimica Acta, 193*(4), 231. https://doi.org/10.1007/s00604-026-07976-x
4. Bobrinetskiy, I., Radovic, M., Rizzotto, F., Vizzini, P., Jaric, S., Pavlovic, Z., Radonic, V., Nikolic, M. V., & Vidic, J. (2021). Advances in nanomaterials-based electrochemical biosensors for foodborne pathogen detection. *Nanomaterials, 11*(10), 2700. https://doi.org/10.3390/nano11102700
5. Chowdhury, A. D., Sarkar, S., Dasgupta, U., & Ghosh, M. (2026). Nanostructured electrochemical biosensors for real-time and portable health monitoring systems. *Biosensors and Bioelectronics X, 30*, 100766. https://doi.org/10.1016/j.biosx.2026.100766

6. Sharma, P., Bhalla, V., Dravid, V., et al. (2012). Enhancing electrochemical detection on graphene oxide-CNT nanostructured electrodes using magneto-nanobioprobes. *Scientific Reports, 2*, 877. https://doi.org/10.1038/srep00877
7. Pandit, S., Li, M., Chen, Y., Rahimi, S., Mokkapati, V., Merlo, A., Yurgens, A., & Mijakovic, I. (2021). Graphene-based sensor for detection of bacterial pathogens. *Sensors, 21*(23), 8085. https://doi.org/10.3390/s21238085
8. Wang, L., Song, N., Zhong, M., & Liu, Z. (2025). Graphene-gold nanoparticle composite-based electrochemical biosensor for human papilomavirus detection. *International Journal of Electrochemical Science, 20*(6), 101014. https://doi.org/10.1016/j.ijoes.2025.101014
9. Arduini, F., Cinti, S., Mazzaracchio, V., Scognamiglio, V., Amine, A., & Moscone, D. (2020). Carbon black as an outstanding and affordable nanomaterial for electrochemical (bio)sensor design. *Biosensors and Bioelectronics, 156*, 112033. https://doi.org/10.1016/j.bios.2020.112033
10. Unser, S., Bruzas, I., He, J., & Sagle, L. (2015). Localized surface plasmon resonance biosensing: Current challenges and approaches. *Sensors, 15*(7), 15684–15716. https://doi.org/10.3390/s150715684
11. Truong, H., Hoang, T., Chung, K., et al. (2025). Plasmonic biosensors and actuators for integrated point-of-care diagnostics. *npj Biosensing, 2*, 45. https://doi.org/10.1038/s44328-025-00050-1
12. Chen, Z., Li, J., Li, T., Fan, T., Meng, C., Li, C., Kang, J., Chai, L., Hao, Y., Tang, Y., Al-Hartomy, O. A., Wageh, S., Al-Sehemi, A. G., Luo, Z., Yu, J., Shao, Y., Li, D., Feng, S., Liu, W. J., He, Y., & Zhang, H. (2022). A CRISPR/Cas12a-empowered surface plasmon resonance platform for rapid and specific diagnosis of the Omicron variant of SARS-CoV-2. *National Science Review, 9*(8), nwac104. https://doi.org/10.1093/nsr/nwac104
13. Zhou, J., Lu, J. Y., Xie, Z. X., Wang, D. H., He, B. S., & Huang, W. T. (2025). Multifunctional Au–Ag–Cr nanocomposites: From multiplex sensing and advanced logic computing to scalable information protection. *Research, 8*, 763. https://doi.org/10.34133/research.0763
14. Subburaj, S., Liu, C., & Xu, T. (2025). Emerging trends in AI-integrated optical biosensors for point-of-care diagnostics: Current status and future prospects. *Chemical Communications, 61*(94), 18464–18489. https://doi.org/10.1039/d5cc04899k

15. Yin, S. (2025). Artificial intelligence-assisted nanosensors for clinical diagnostics: Current advances and future prospects. *Biosensors, 15*(10), 656. https://doi.org/10.3390/bios15100656
16. Wasilewski, T., Kamysz, W., & Gębicki, J. (2024). AI-assisted detection of biomarkers by sensors and biosensors for early diagnosis and monitoring. *Biosensors, 14*(7), 356. https://doi.org/10.3390/bios14070356
17. Lee, S., Moussa, N. A. M., & Kang, S. H. (2025). Deep learning-enhanced nanozyme-based biosensors for next-generation medical diagnostics. *Biosensors, 15*(9), 571. https://doi.org/10.3390/bios15090571
18. Kumar, S., & Khan, Y. U. (2023). Biomedical signals classification with transformer based model. In *2023 International Conference on Power, Instrumentation, Energy and Control (PIECON)*. IEEE. https://doi.org/10.1109/PIECON56912.2023.10085908
19. Bocan, A., Moakhar, R. S., Del Real Mata, C., Petkun, M., De Iure-Grimmel, T., Yedire, S. G., Shieh, H., Khorrami Jahromi, A., Mahshid, S. S., & Mahshid, S. (2025). Machine-learning-aided advanced electrochemical biosensors. *Advanced Materials, 37*(33), e2417520. https://doi.org/10.1002/adma.202417520
20. Nashruddin, S. N. A. B. M., Salleh, F. H. M., Yunus, R. M., & Zaman, H. B. (2024). Artificial intelligence-powered electrochemical sensor: Recent advances, challenges, and prospects. *Heliyon, 10*(18), e37964. https://doi.org/10.1016/j.heliyon.2024.e37964
21. Geddis, A., Williams, H., Bashir, S., Malenfant, J., Dubois, C., Hamlet, L., & Masson, J. (2026). Artificial intelligence and machine learning for plasmonic and surface-enhanced sensing. *Chemical Society Reviews*, *55*(6), 3599–3644. https://doi.org/10.1039/d5cs01522g
22. Chowdhury, A. D., Sarkar, S., Dasgupta, U., & Ghosh, M. (2026). Nanostructured electrochemical biosensors for real-time and portable health monitoring systems. *Biosensors and Bioelectronics X, 30*, 100766. https://doi.org/10.1016/j.biosx.2026.100766
23. Cao, M., Deng, W., Zhu, Z., Ma, C., Bai, J., Emran, M. Y., Kotb, A., Sun, M., & Zhou, M. (2024). A fully integrated handheld electrochemical sensing platform for point-of-care testing of *Escherichia coli* O157:H7. *Analytical Chemistry, 96*(13), 5340–5347. https://doi.org/10.1021/acs.analchem.4c00776

24. Liu, G., Guan, X., Zhang, P., Tan, Q., Li, T., Jin, X., & Zhao, J. (2025). A fully integrated wearable microfluidic electrochemical sensor with ultrasonic connecting and hot-pressing bonded multilayer structure for sweat biomarker analysis. *Analytical Chemistry*, *97*(41), 22858–22870. https://doi.org/10.1021/acs.analchem.5c04641
25. Anuthra, B., Ratan, J., Gupta, P., et al. (2026). Advances in low-cost electrochemical sensors for healthcare monitoring and diagnostics. *Advanced Industrial Engineering Chemistry*, *2*, 3. https://doi.org/10.1007/s44405-026-00043-2
26. Dong, T., Pires, N. M. M., Yang, Z., & Jiang, Z. (2022). Advances in electrochemical biosensors based on nanomaterials for protein biomarker detection in saliva. *Advanced Science*, *10*(6), e2205429. https://doi.org/10.1002/advs.202205429
27. Tang, Y., Li, Y., Chen, P., Zhong, S., & Yang, Y. (2025). Nucleic acid aptamer-based sensors for bacteria detection: A review. *BioEssays*, *47*(3), e202400111. https://doi.org/10.1002/bies.202400111
28. Li, T., Xiao, L., Ling, H., Yang, Y., & Zhong, S. (2025). Preparation of artificial substrate binding sites of nanozyme with "modular structure" strategy used for the construction of visual sensing analysis platform for levodopa. *Microchemical Journal*, *212*, 113292. https://doi.org/10.1016/j.microc.2025.113292
29. Gao, S., Chang, H., Wang, C., Chi, M. P., Lin, C., Chiang, C., Wang, C., Huang, C., Li, P., & Chau, L. (2025). Oriented immobilization of antibodies on suspended nanoparticle and substrate surfaces via one-step catch-and-link approach for development of biosensors. *Microchemical Journal*, *210*, 112967. https://doi.org/10.1016/j.microc.2025.112967
30. Wang, B., Wang, H., Lu, X., Zheng, X., & Yang, Z. (2023). Recent advances in electrochemical biosensors for the detection of foodborne pathogens: Current perspective and challenges. *Foods*, *12*(14), 2795. https://doi.org/10.3390/foods12142795
31. Banakar, M., Hamidi, M., Khurshid, Z., Zafar, M. S., Sapkota, J., Azizian, R., & Rokaya, D. (2022). Electrochemical biosensors for pathogen detection: An updated review. *Biosensors*, *12*(11), 927. https://doi.org/10.3390/bios12110927
32. Ma, H., Li, G., Zhang, H., Wang,X., Li, F., Yan, J., Hong, L., Zhang, Y., & Pu, Q. (2025). Rapid and ultra-sensitive detection of foodborne pathogens by deep learning-enhanced microfluidic biosensing. *Sensors and Actuators B: Chemical*, *436*, 137646. https://doi.org/10.1016/j.snb.2025.137646

33. Mahek Sadiq, Q. N. K. Hoang, A. Kishlock, F. G. Sabzevari, K. Katti, D. Katti, Q. Zhang, & D. Wang. (2024). MXene-montmorillonite nanocomposites-based scaffold sensors for early pancreatic cancer diagnosis. *Cancer Plus, 6*(3), 3793. https://doi.org/10.36922/cp.3793
34. Jiang, W., Liu, L., & Bu, Y. (2025). Application of deep learning in the phase processing of digital holographic microscopy. *Photonics, 12*(8), 810. https://doi.org/10.3390/photonics12080810
35. Wang, S., Zheng, C., Ma, T., Wang, T., Gao, S., Dai, Q., & Chu, F. (2024). Tooth backlash inspired comb-shaped single-electrode triboelectric nanogenerator for self-powered condition monitoring of gear transmission. *Nano Energy, 123*, 109429. https://doi.org/10.1016/j.nanoen.2024.109429